Online vehicle aerodynamic drag observer with Kalman filters

Youssef El Gaouti, Guillaume Colin, B Thiam, Nicolas Mazellier

Online vehicle aerodynamic drag observer with Kalman filters

Y. El Gaouti * **G. Colin** * **B. Thiam** * **N. Mazellier** *

* *Laboratoire PRISME - Univ. Orléans, 8, rue Léonard de Vinci, 45072 Orléans, France*

(youssef.elgaouti@gmail.com, guillaume.colin@univ-orleans.fr)

Abstract: Aerodynamic drag is an important contributor to vehicle energy consumption, especially in highway conditions. Hence, estimating on-line the aerodynamic drag, or equivalently its coefficient, is an interesting challenge in order to reduce the energy consumption of vehicles. However, real systems are characterized by noisy sensor measurements. Extended Kalman Filter (EKF) is a commonly used algorithm for parameter estimation due to its stochastic filtering properties and is based on a first order approximation of the system dynamics. Similarly, the Unscented Kalman Filter (UKF) has been proposed as an alternative to the EKF in the field of nonlinear filtering and has received great attention in parameter estimation. This paper presents these two observers EKF and UKF for online estimation of the aerodynamic drag coefficient, based on noisy sensor measurements of a vehicle velocity, powertrain wheel torque and a longitudinal dynamic vehicle model. The design of the estimators is described and the performances are assessed against real measurements. The robustness is evaluated with different spoiler positions and the optimal position corresponding to a minimum of the aerodynamic drag coefficient is confirmed. Two different masses are used to validate each estimator.

Keywords: Drag vehicle, Observer, Extended Kalman Filter, Unscented Kalman Filter, Nonlinear System, Experimental results.

1. INTRODUCTION

In the field of transportation, commercial vehicles, buses, semi-tractors and cars are large fuel consumers and pollutant emitters. Recently, the European Parliament and Council adopted regulation on CO_2 emissions for new passenger cars and for new light-duty commercial vehicles (European Commission, 2019). To address these issues, researchers were interested in mitigating aerodynamic drag in order to reduce fuel consumption and hence CO_2 emissions. In the field of fluid mechanics, drag is reduced by controlling the flow, e.g. by using a vortex generator (VG) or spoilers (Bansal and Sharma, 2014; Ajitanshu and Dheeraj, 2018). The optimal conditions are found with the minimum drag coefficient. Calculating this coefficient online is not straightforward, however. In this paper, a vehicle is equipped with spoilers that make the drag coefficient vary. In automotive sector, the aerodynamic drag coefficient is generally estimated offline using the coast down test (White and Korst, 1972) or with wind-tunnel experiments (Walter et al., 2001). Here, we focus on an online estimation of the drag coefficient.

The aerodynamic drag, rolling resistance, vehicle mass and road grade can be used together with a longitudinal model to estimate the vehicle power demands, but these parameters are often subject to change. For example with the variation in the passenger number or the payload, the vehicle mass can change. The rolling resistance depends on tires and road conditions, and the aerodynamic drag can change as a function of the vehicle mass and flow control (e.g. with a spoiler). It is therefore necessary to estimate these parameters online for conventional vehicles. In (Vahidi et al., 2005) Recursive least squares with forgetting was investigated to estimate online the vehicle mass and road grade. (Sahlholm and Henrik Johansson, 2010) presented an experimental study, using a Kalman filter to estimate the road grade coefficient. The extended Kalman filter and the linear Kalman filter were used in (Andersson, 2012) to estimate the aerodynamic drag and the rolling resistance. Similarly a model-based estimation for Vehicle Aerodynamic Drag and Rolling Resistance was presented in (Zhang et al., 2015), this technique makes it possible to estimate the two parameters together. In the same way, (Trigui et al., 2016) compared two methods of estimating the electric vehicle rolling resistance coefficient, namely recursive least squares and neural network, in winter conditions.

In this paper we propose two methods, the extended and unscented Kalman filters, for online estimation of the aerodynamic drag coefficient. They both use the augmented longitudinal vehicle model in discrete time and the measured signals obtained with the Control Area Network (CAN) bus. The first method uses the linearized model, while the second method investigates the nonlinear model directly that can remove the error from the linearizing procedures.

The rest of this document is organized as follows. The nonlinear vehicle model is described in Section 2 and its observability discussed in section 3. In Section 4, the two

observers designed for this application are presented. Section 5 presents experimental results and compares different driving conditions : two vehicle masses and five positions of the spoiler. In light of the results, conclusions and perspectives are drawn on the problem under consideration.

2. VEHICLE MODEL

The vehicle dynamics is modeled on the longitudinal axis. Vehicle motion is the result of the forces applied on its body. According to Newton's law of motion, the vehicle speed v satisfies the following differential equation:

$$\dot{v}(t) = \frac{1}{m}(F_{pwt}(t) - F_{gravity} - F_{rol} - F_{dd}(t)), \quad (1)$$

where $\dot{()}$ denotes the time derivative, and m the vehicle equivalent mass. The traction force of the vehicle F_{pwt} can be calculated as follows

$$F_{pwt}(t) = \frac{\eta_{gb} R_{gb} R_t}{r_{tire}} T_c(t), \quad (2)$$

where R_{gb} is the gear-box ratio, η_{gb} the gear-box efficiency, R_t the differential ratio, r_{tire} the wheel radius [m] and T_c the wheel torque [Nm].

The aerodynamic drag force F_{dd} can be calculated as

$$F_{dd}(t) = \frac{1}{2}\rho c_d S v^2(t), \quad (3)$$

with S the vehicle frontal area [m^2], ρ the air density and c_d the aerodynamic drag coefficient.

The rolling resistance F_{rol} can be calculated as

$$F_{rol} = mgc_r \cos(\alpha) \approx mgc_r. \quad (4)$$

A constant value of c_r is often adequate for the rolling resistance estimation. In (4), α represents the road slope and g the gravity constant [m/s^2]. The road grade force $F_{gravity}$ can be calculated as

$$F_{gravity} = mg \sin \alpha. \quad (5)$$

Continuous augmented state space form

The parameter c_d is estimated by augmenting the vehicle model (1) with one state corresponding to the parameter to be estimated. The parameter c_d is assumed to change slowly in comparison to the vehicle speed; its derivatives are therefore approximated to zero $\dot{c}_d(t) = 0$ (Gustafsson, 2001; Höckerdal, 2011). Augmenting the vehicle model thus yields the following process model:

$$\begin{bmatrix} \dot{v}(t) \\ \dot{c}_d(t) \end{bmatrix} = \begin{bmatrix} \frac{1}{m}(F_{pwt}(t) - F_{gravity} - F_{rol} - F_{dd}(t)) \\ 0 \end{bmatrix} \quad (6)$$

In summary, the complete vehicle model in the continuous state space form reads as:

$$\begin{cases} \dot{x}(t) = f(x(t), u(t)) \\ y(t) = h(x(t)) \end{cases} \quad (7)$$

In this paper, we chose $u(t)$ as the powertrain wheel torque $T_c(t)$.

Discrete state space form

To obtain the discrete form representation of system (6), a zero-order-hold assumption for the system input vector $u(t)$ during the sampling time T_0 was used. This allows us to apply the Taylor-Lie series discretization approach (Kazantzis and Kravaris, 1997) in the form:

$$x_i(k+1) = x_i(k) + \sum_{i=1}^{N_i} (L_f^l x_i)|_{x(k),u(k)} \frac{T_0^l}{l!}, \quad (8)$$

Here, k refers to the discrete time step, $i = 1, 2$ denotes the i^{th} element of the state vector x, N_i is the truncation order of the Taylor-Lie series, and $L_f^l x_i$ is the lth order Lie derivative of x_i along the vector field f. In order to reduce the computational effort, the Taylor-Lie series of order $N = 1$ is used for the states v and c_d. This choice corresponds to the classical forward Euler integration since $u(k)$ is constant due to the zero-order-hold assumption. Introducing the stochastic process noise ω and the stochastic measurement noise b, we obtain the final system description for the filter design in the form:

$$\begin{cases} x_{k+1} = f(x_k, u_k) + w_k \\ y_k = h(x_k) + b_k \end{cases}, \quad (9)$$

where $h(x_k)$ is the measurement equation equal to vehicle speed at time k.

In (9), the measured output y is the vehicle speed, the states x are vehicle speed v and drag coefficient c_d and the input is the powertrain wheel torque T_c.

3. OBSERVABILITY OF THE NONLINEAR SYSTEM

In this section, we employ the observability rank criterion based on Lie derivatives to verify the conditions under which the nonlinear system that describes the process of the vehicle is observable. For a nonlinear system, the observability matrix O can be calculated as the Jacobian of the matrix spanned by the Lie derivative L along the vector field f:

$$O = \begin{bmatrix} dh \\ dL_f h \\ \vdots \\ \vdots \\ dL_f^{n-1} h \end{bmatrix} = \begin{bmatrix} 1 & 0 \\ \frac{1}{m} S\rho c_d v & -\frac{1}{2m} S\rho c_d v^2 \end{bmatrix}. \quad (10)$$

The elements of the observability matrix of our system (Boutat, 2014) are written as follows:

$$dh = (\frac{\partial h}{\partial x_1}, \frac{\partial h}{\partial x_2}, ..., \frac{\partial h}{\partial x_n}), \quad (11)$$

where dh is the differential of h. $L_f h$ is called the Lie derivative of h in the direction of f:

$$L_f h = f_1 \frac{\partial h}{\partial x_1} + f_2 \frac{\partial h}{\partial x_2} + ... + f_n \frac{\partial h}{\partial x_n}, \quad (12)$$

where the writing of $dL_f^k h$ here is given by the co-vector:

$$dL_f^k h = (\frac{\partial L_f^k h}{\partial x_1}, \frac{\partial L_f^k h}{\partial x_2}, ..., \frac{\partial L_f^k h}{\partial x_n}). \quad (13)$$

As for linear systems, if the matrix O has full column rank, then the system is said to be observable:

$$rank(O) = n \quad (14)$$

By performing the calculations and applying the observability criterion (14) it can be shown that the system is observable as long as the vehicle speed is nonzero.

4. OBSERVER DESIGN

A common method for parameter estimation is to use an observer based on a state space representation. This estimator can be used to reconstruct the states of a system that cannot be measured (Simon, 2006). Estimations of the system internal states can be made based on knowledge of the system's input and output signals.

4.1 Extended Kalman Filter (EKF)

The Kalman filter is used as a state observer in the field of linear system. It estimates the state of the real system indirectly, by approximating the statistic properties of the random variables. An extension of this observer is the extended Kalman filter, in the case of nonlinear processes. To tackle the nonlinear problem, the extended Kalman filter linearizes the nonlinear function f in time $k-1$ and predicts the image in time k. EKF uses the nonlinear representation of the process model in the time update equation for the estimated states (Simon, 2006). The estimation is done in two steps: the time update equations and the measurement update equations. The notation $x_{k|k-1}$ is used to indicate the state x at time k given the information up until time $k-1$. The time update equations predict the estimated states $\hat{x}_{k|k-1}$ and estimated error covariance $P_{k|k-1}$ for the next time step; the global algorithm is given by:

$$\begin{cases} \hat{x}_{k|k-1} = f(\hat{x}_{k-1|k-1}, u_k), \\ P_{k|k-1} = F_k P_{k-1|k-1} F^T + Q_k, \end{cases} \tag{15}$$

where $F_k = \frac{\partial f}{\partial x}(\hat{x}_{k-1|k-1}, u_k)$.

The measurement update equations are used to correct the estimated states and error covariance predicted in the time update equations by comparing the estimated states with the measurements:

$$\hat{x}_{k|k} = \hat{x}_{k|k-1} + K_k(y_k - H_k \hat{x}_{k|k-1}), \tag{16}$$

with

$$K_k = P_{k|k-1} H_k^T (H_k P_k H_k^T + R_k)^{-1}, \tag{17}$$

and

$$P_{k|k} = (I - K_k H_k) P_{k|k-1}, \tag{18}$$

where Q_k and R_k are positive definite matrices that represent respectively the covariance of process noise and measurement noise. H_k is the Jacobian of $h(x_k)$. Note that all the process noise and measurement noise used in Kalman filters are white Gaussian noise as well as independent from each other. This is an essential condition for the estimator to converge.

4.2 Unscented Kalman Filter (UKF)

Another application of Kalman ideas to the state estimation of nonlinear systems is the UKF. The UKF also approximates the statistic properties of the random variables up to the second order. In contrast to EKF and the standard Kalman filter for linear systems, it is not the mean value and covariance but a minimal set of carefully chosen weighted sample points, the so-called sigma points, that are used for the approximation. These points are chosen as $2n+1$, where n given in (Chowdhary and Jategaonkar, 2006) as the total number of augmented states to be estimated. More details can be found in (Antonov et al., 2011), (Wan and Van Der Merwe, 2000).

Before giving the algorithm of UKF we have to define the weighted sigma points as:

$$w_0 = \frac{\kappa}{\kappa + n} \quad \text{and} \quad w_i = \frac{1}{2(\kappa + n)} \quad \text{for} \quad i = 1, ..., 2n, \tag{19}$$

where κ provides an extra degree of freedom, and can be used to reduce the overall prediction errors. A useful heuristic is to select $n + \kappa = 3$ (Julier and Uhlmann, 1997).

There are two steps for the UKF algorithm, the first is the prediction and the second is the update.

1^{st} *step: Prediction*

$$\begin{aligned} \chi^x(k|k) = [&\hat{x}(k|k), \hat{x}(k|k) + \eta\sqrt{P_x(k|k)}, \hat{x}(k|k) \\ &- \eta\sqrt{P_x(k|k)}], \end{aligned} \tag{20}$$

$$\chi_i^x(k+1|k) = f(\chi_i^x(k|k), u(k)), \tag{21}$$

$$\hat{x}(k+1|k) = \sum_{i=0}^{2n} w_i \chi_i^x(k+1|k), \tag{22}$$

$$\begin{aligned} P_x(k+1|k) = &\sum_{i=0}^{2n} w_i (\chi_i^x(k+1|k) - \hat{x}(k+1|k)) \\ &(\chi_i^x(k+1|k) - \hat{x}(k+1|k))^T + R_k. \end{aligned} \tag{23}$$

2^{th} *step: Measurement update*

$$\begin{aligned} \chi^*(k|k) = [&\hat{x}(k+1|k), \hat{x}(k+1|k) + \eta\sqrt{P_x(k|k)}, \hat{x}(k+1|k) \\ &- \eta\sqrt{P_x(k|k)}], \end{aligned} \tag{24}$$

$$\gamma_i^y(k+1|k) = h(\chi_i^*(k+1|k)), \quad , \tag{25}$$

$$\hat{y}(k+1|k) = \sum_{i=0}^{2n} w_i \gamma_i(k+1|k), \tag{26}$$

$$\begin{aligned} P_y(k+1|k) = &\sum_{i=0}^{2n} w_i (\gamma_i(k+1|k) - \hat{y}(k+1|k)) \\ &(\gamma_i(k+1|k) - \hat{y}(k+1|k))^T + Q_k, \end{aligned} \tag{27}$$

$$\begin{aligned} P_{xy}(k+1|k) = &\sum_{i=0}^{2n} w_i (\chi_i(k+1|k) - \hat{x}(k+1|k)) \\ &(\gamma_i(k+1|k) - \hat{y}(k+1|k))^T, \end{aligned} \tag{28}$$

$$K(k+1) = P_{xy}(k+1|k) P_y(k+1|k)^{-1}, \tag{29}$$

$$\begin{aligned} \hat{x}(k+1|k+1) = &\hat{x}(k+1|k) + K(k+1)(y(k+1|k) \\ &- \hat{y}(k+1|k)), \end{aligned} \tag{30}$$

$$P_x(k+1|k+1) = P_x(k+1|k) - K(k+1) \\ P_y(k+1|k)K(k+1)^T. \quad (31)$$

4.3 Tuning of the observers

The tuning of the variance and covariance matrices Q, R and P is an essential point during the implementation of a Kalman filter. Firstly, we choose an arbitrary tuning to select the following process noise covariance, measurement noise variance and initial value for the estimated error covariance in order to obtain a good convergence of the estimates of speed and drag coefficient towards their real values. Recall that these parameters are related to the variance of random noise that is difficult to quantify. However we can neglect the influence of correlation between the different noises as a first simplification and thus have symmetric matrices defined positive. In the case of a nonlinear Kalman filter, the matrix P_0 essentially determines the initial dynamics of the filter, which is not of great importance for an online application. On the other hand, an incorrect setting of P_0 can compromise the stability of a Kalman filter.

For each estimator, Q , R and P are chosen as

$$Q_K = \begin{bmatrix} 10^{-3} & 0 \\ 0 & q_{22} \end{bmatrix} \quad (32)$$

$$R_K = 10^{-4} \quad (33)$$

$$P_0 = \begin{bmatrix} 10^{-3} & 0 \\ 0 & 10^{-1} \end{bmatrix} \quad (34)$$

Three values of q_{22} will be used in the following: 10^{-6}, 10^{-7}, 10^{-8} that define respectively dynamic, compromise and slow tuning for drag coefficient estimation.

5. EXPERIMENTAL RESULTS

Experimental data were acquired from real-world driving tests to assess the estimator performance. From an electrical vehicle with two different masses, the vehicle rolling resistance coefficient c_r was identified to 0.007 and the sampling time was set to 0.01s. The tests were done on a regular road which implies considering the road-grade equal to zero. To validate the proposed aerodynamic drag estimation, two vehicle mass tests were achieved, and for each vehicle mass five tests were done with different spoiler positions. Real-time simulations were performed using Matlab.

5.1 Offline estimation

Two classical ways are used to estimate offline the aerodynamic drag coefficient. The first solution is the use of a wind tunnel (Walter et al., 2001), not shown here. The second one (White and Korst, 1972), shown here, launches the vehicle at a given speed in neutral gear (so $T_c(t) = 0$) and the aerodynamic drag coefficient is identified with the classical least square method. This estimation is noted $\hat{c}_d$. Fig. 1 and 2 show the results for two vehicle masses. We see the effect of the spoiler on the aerodynamic drag $\hat{c}_d$. The variation of $\hat{c}_d$ between the two masses is due to the fact that neither the vehicle mass nor the rolling resistance coefficient were changed during the identification to be able to compare with the online estimation. With these tests, we see that the optimal spoiler position seems to be around 15°. Note that the real value of the aerodynamic drag coefficient has been changed for confidential reasons, and some spoiler positions are missing due to experimental problems.

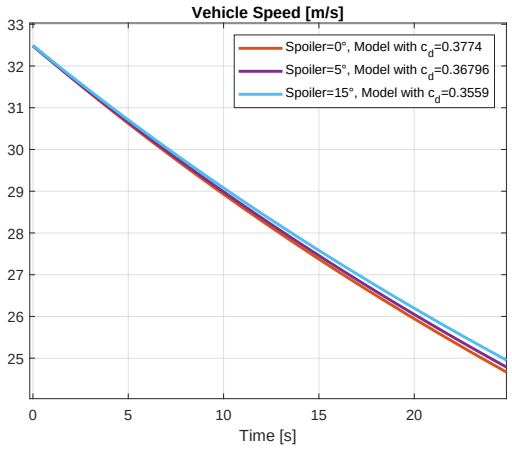

Fig. 1. Deceleration experiments for different spoiler positions with vehicle mass=1764kg

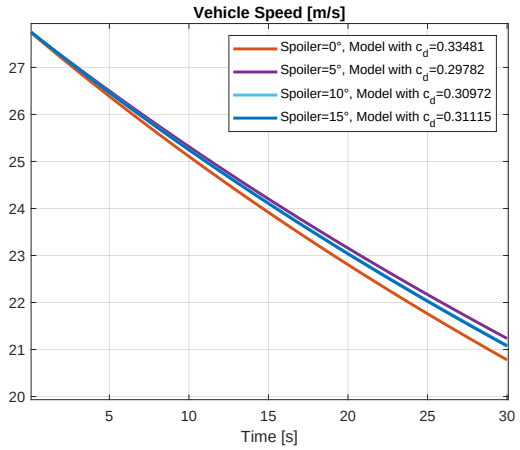

Fig. 2. Deceleration experiments for different spoiler positions with vehicle mass=1950kg

5.2 Online estimation

To assess the robustness of the drag estimator, an add-on protuberance (foam placed at the rear of the vehicle) was implemented with the purpose of impacting the aerodynamic performance of the vehicle.

Fig. 3 shows an example of the real data (vehicle speed and torque versus time) obtained for the vehicle mass m=1764kg, used for our estimation algorithm. We present five curves for different spoiler positions from 0° to 15°, and also with the protuberance at the rear of the vehicle. These experiments change the aerodynamic drag resistance, which is opposed to the vehicle movement.

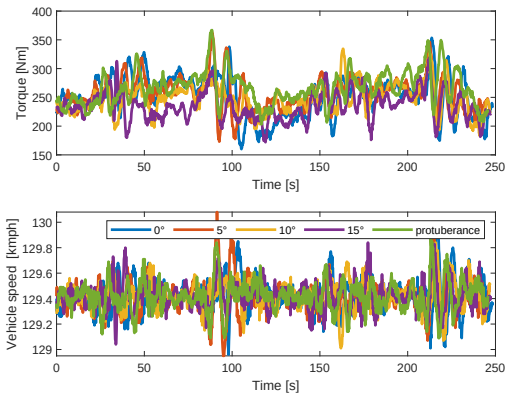

Fig. 3. Torque [Nm] (top) and vehicle speed [kmph] (bottom) versus time [s] for vehicle mass m=1764kg for different spoiler positions

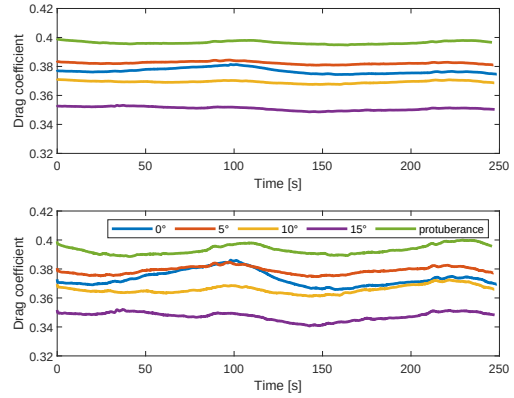

Fig. 4. UKF Drag coefficient estimation with compromise (bottom) and slow (top) tuning versus time [s] for a vehicle mass m=1764kg

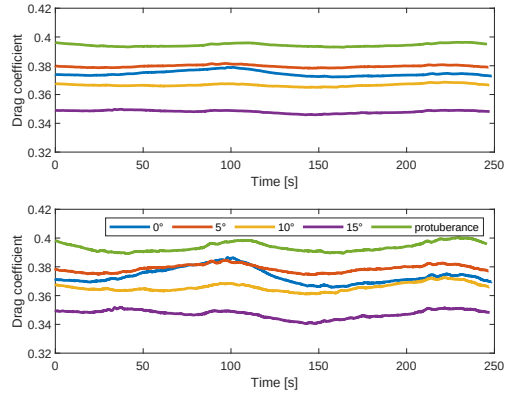

Fig. 5. EKF Drag coefficient estimation with compromise (bottom) and slow (top) tuning versus time [s] for a vehicle mass m=1764kg

Our proposed drag coefficient estimation algorithm was evaluated by simulations, carried out using Matlab.

Thus, Fig. 4 shows the efficiency of the UKF estimator with compromise (bottom) and slow tuning (top) for q_{22} (32). As we can see in the upper figure, the coefficient obtained with a vehicle equipped with foam converges near to 0.4, and decreases with spoiler position, except for position 5°, which converges near to 0.381. We can also note that the slow tuning smoothes out the dynamics. In the same way we conclude from Fig. 5 that the EKF also converges to almost the same value.

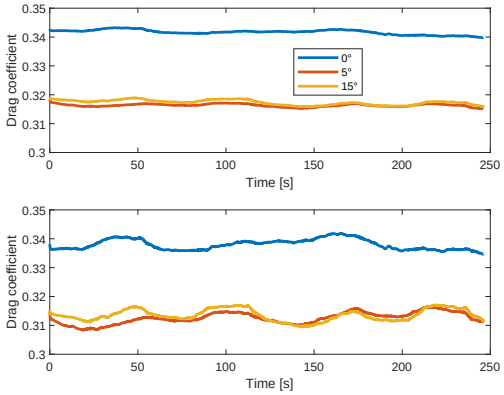

Fig. 6. UKF Drag coefficient estimation with compromise (bottom) and slow (top) tuning versus time [s] for a vehicle mass m=1950kg

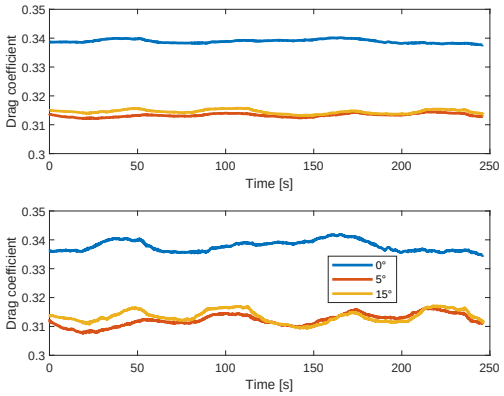

Fig. 7. EKF Drag coefficient estimation with compromise (bottom) and slow (top) tuning versus time [s] for a vehicle mass m=1950kg

Similarly, Fig. 6 and 7 show the simulation results for the vehicle mass m=1950kg with different spoiler positions from 0° to 15°. We can note that both EKF and UKF give similar results.

To sum up, Table 1 shows the average estimation of the drag coefficient obtained for each experiment and both observers (UKF and EKF). This table shows that both estimators could be used for online vehicle drag estimation. Finally, the experiments show that the optimal spoiler position is here 15°. The estimated drag coefficient obtained in deceleration measurements is very close to the value obtained by Kalman filters.

Fig. 8 shows a comparison of the estimator response from all three different tunings of the UKF and spoiler position versus time for a vehicle mass=1764kg. This shows that the UKF is able to estimate the drag coefficient while the spoiler varies but that the filter tuning has a great impact on the results obtained.

6. CONCLUSION

The drag coefficient for an electrical vehicle has been estimated, and the effect of the spoiler position has been

Table 1. Comparison of drag coefficient estimation average obtained with a slow tuning of both filters and $\hat{c}_d$ obtained with the offline estimation

	$m = 1764kg$			$m = 1950kg$		
Spoiler	UKF	EKF	$\hat{c}_d$	UKF	EKF	$\hat{c}_d$
0°	0.377	0.375	0.377	0.342	0.339	0.335
5°	0.382	0.380	0.368	0.316	0.313	0.298
10°	0.369	0.367	-	-	-	0.309
15°	0.351	0.348	0.356	0.317	0.314	0.311
add-on	0.396	0.394	-	-	-	-

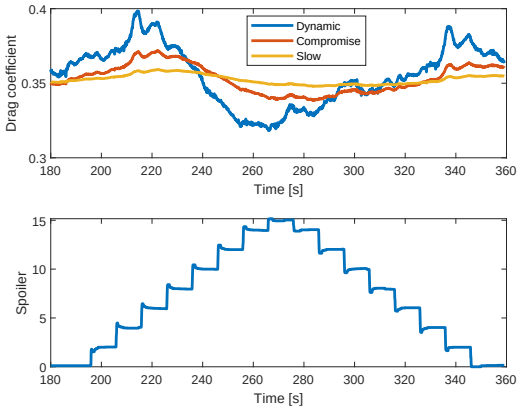

Fig. 8. Three different tunings of the UKF Drag coefficient estimation (top) and Spoiler position [deg] (bottom) versus time [s] for a vehicle mass=1764kg

discussed. Two nonlinear estimators EKF and UKF have been investigated to solve the problem of aerodynamic drag estimation. Additionally, the impact of the spoiler position for the aerodynamic drag coefficient has been studied. Based on real data measurements for two cars of different weights, it is shown that it is possible to find an optimal angle in order two improve fuel consumption and vehicle control.

In future work, the estimator will be implemented to obtain the optimal conditions for other actuators (vortex generator and others spoilers) in order to improve vehicle energy economy and thus decrease CO_2 emissions.

REFERENCES

Ajitanshu, V. and Dheeraj, S. (2018). Experimental and simulation studies on aerodynamic drag reduction over a passenger car. *International Journal of Fluid Mechanics Research, 46*, 67(1), 39—-61. doi: 10.1615/InterJFluidMechRes.2018025171.

Andersson, R. (2012). *Online Estimation of Rolling Resistance and Air Drag for Heavy Duty Vehicles*. Master Sci Thesis. 2012.

Antonov, S., Fehn, A., and Kugi, A. (2011). Unscented Kalman filter for vehicle state estimation. *Vehicle System Dynamics*, 49(9), 1497–1520. doi: 10.1080/00423114.2010.527994.

Bansal, R. and Sharma, R.B. (2014). Drag reduction of passenger car using add-on devices. *Journal of Aerodynamics*, 13, 1—-13. doi:10.1155/2014/678518.

Boutat, D. (2014). La notion d'observateur pour les systèmes non linéaires. *Cours d'école Doctorale d'Orléans : Sciences et Technologies*.

Chowdhary, G. and Jategaonkar, R. (2006). Aerodynamic Parameter Estimation from Flight Data Applying Extended and Unscented Kalman Filter. In *AIAA Atmospheric Flight Mechanics Conference and Exhibit*. American Institute of Aeronautics and Astronautics, Keystone, Colorado. doi:10.2514/6.2006-6146.

European Commission (2019). Post-2020 co_2 emission performance standards for cars and vans.

Gustafsson, F. (2001). *Adaptive Filtering and Change Detection*. John Wiley & Sons, Ltd, Chichester, UK. doi:10.1002/0470841613.

Höckerdal, E. (2011). *Model Error Compensation in ODE and DAE Estimators*. Doctoral thesis, Linköping University, Linköping, Sweden.

Julier, S.J. and Uhlmann, J.K. (1997). New extension of the Kalman filter to nonlinear systems. In I. Kadar (ed.), *AeroSense '97*, 182. Orlando, FL, USA. doi: 10.1117/12.280797.

Kazantzis, N. and Kravaris, C. (1997). System-theoretic properties of sampled-data representations of nonlinear systems obtained via Taylor-Lie series. *International Journal of Control*, 67(6), 997–1020. doi: 10.1080/002071797223901.

Sahlholm, P. and Henrik Johansson, K. (2010). Road grade estimation for look-ahead vehicle control using multiple measurement runs. *Control Engineering Practice*, 18(11), 1328–1341. doi: 10.1016/j.conengprac.2009.09.007.

Simon, D. (2006). *Optimal State Estimation: Kalman, H* inf *and Nonlinear Approaches*. Wiley-Interscience, Hoboken, N.J. OCLC: ocm64084871.

Trigui, O., Dube, Y., Kelouwani, S., and Agbossou, K. (2016). Comparative Estimation of Electric Vehicle Rolling Resistance Coefficient in Winter Conditions. In *2016 IEEE Vehicle Power and Propulsion Conference (VPPC)*, 1–6. IEEE, Hangzhou, China. doi: 10.1109/VPPC.2016.7791630.

Vahidi, A., Stefanopoulou, A., and Peng, H. (2005). Recursive least squares with forgetting for online estimation of vehicle mass and road grade: Theory and experiments. *Vehicle System Dynamics*, 43(1), 31–55. doi: 10.1080/00423110412331290446.

Walter, J.A., Pruess, D.J., and Romberg, G.F. (2001). Coastdown/Wind Tunnel Drag Correlation and Uncertainty Analysis. In *SAE 2001 World Congress*, 2001–01–0630. doi:10.4271/2001-01-0630.

Wan, E. and Van Der Merwe, R. (2000). The unscented Kalman filter for nonlinear estimation. In *Proceedings of the IEEE 2000 Adaptive Systems for Signal Processing, Communications, and Control Symposium (Cat. No.00EX373)*, 153–158. IEEE, Lake Louise, Alta., Canada. doi:10.1109/ASSPCC.2000.882463.

White, R.A. and Korst, H.H. (1972). The determination of vehicle drag contributions from coast-down tests. *SAE Technical Paper 720099*, 6.

Zhang, D., Ivanco, A., and Filipi, Z. (2015). Model-Based Estimation of Vehicle Aerodynamic Drag and Rolling Resistance. *SAE International Journal of Commercial Vehicles*, 8(2), 433–439. doi:10.4271/2015-01-2776.